



Synthesis, characterization, *in silico* DNA studies and antibacterial evaluation of transition metal complexes of thiazole based pyrazolone Schiff base

J. Senthil Kumaran^{a†}, J. Muthukumar^b, N. Jayachandramani^c and S. Mahalakshmi^c

^aDepartment of Chemistry, Sriram College of Arts and Science, Perumalpattu, Thiruvallur, Tamil Nadu, India

^bUCIBIO, REQUIMTE, Faculdade de Ciências e Tecnologia, Universidade Nova de Lisboa, Caparica, Portugal

^cPG & Research Department of Chemistry, Pachaiyappa's College, Chennai, Tamil Nadu, India

ABSTRACT

A new series of transition metal complexes of Schiff base ligand containing 4-hydroxy-3-methoxybenzaldehyde (vanillin), 4-aminoantipyrine and 2-aminothiazole have been synthesized. All the complexes have been characterized by the use of elemental analyses, molar conductance values, magnetic moments, FT-IR, ¹H-NMR, Mass and electronic absorption data. The Schiff base is found to act as tridentate ligand leading to an octahedral geometry of the complexes. The ESR spectra of copper complex in Tetracyanoethylene (TCNE) solution were recorded at room temperature (RT) and liquid nitrogen temperature (LNT) and its significant features are reported. The redox behavior of the copper complex at RT was well studied. The *in silico* DNA results revealed that cobalt and copper complexes are bound to the "Minor groove" and nickel and zinc complexes are bound to the "Major groove" portion of DNA through hydrogen bonds and hence they are called "Minor groove and Major groove binders" respectively. The Schiff base and its metal complexes have been screened for their *in vitro* antibacterial activities.

Key words: Metal complexes, 4-aminoantipyrine, ESR spectra, *in silico* DNA study, antibacterial activity

INTRODUCTION

The Schiff bases play a momentous role in the development of coordination chemistry as they easily form stable complexes with most metals in different oxidation states [1] and they are most extensively used ligands due to the easy synthesis procedure, remarkable expediency and good solubility in common solvents. The Schiff bases have been the subject of huge attention for a number of years because of their an assortment of chemical and structural characteristics and also their showed applications as biologically active molecules and these complexes are known to be biologically vital and act as models to understand the structure of biomolecules and metallo proteins [2,3]. Many studies suggest that DNA is the primary intracellular target of antitumor drugs because the interaction between small molecules and DNA can cause DNA damage in cancerous cells [4-6]. The binding mechanism of metal complexes of DNA were studied in order to develop new potential DNA targeting antitumor drugs.

It has been proved that Schiff bases of 4-aminoantipyrine and its complexes have a wide application in medicine, analytical and pharmacological areas [7,8]. Thiazoles possess a broad range of antitumour, antibiotic, antibacterial, antifungal and anti-inflammatory activities [9-12]. The above specific details were kept in mind and thereby the aim of this work is to synthesize and characterize novel Cu (II), Co (II), Ni (II) and Zn (II) complexes of Schiff base ligand derived from 4-aminoantipyrine, 4-hydroxy-3-methoxybenzaldehyde and 2-aminothiazole. The structure of

synthetic compounds was elucidated by using elemental analyses, magnetic moment, Mass, IR, $^1\text{H-NMR}$, Cyclic Voltammetric technique, ESR and electronic absorption spectroscopy. The theoretical DNA studies and antimicrobial activities of the metal complexes has also been carried out for understanding the biological activities of the synthetic compounds.

EXPERIMENTAL SECTION

2.1. Materials

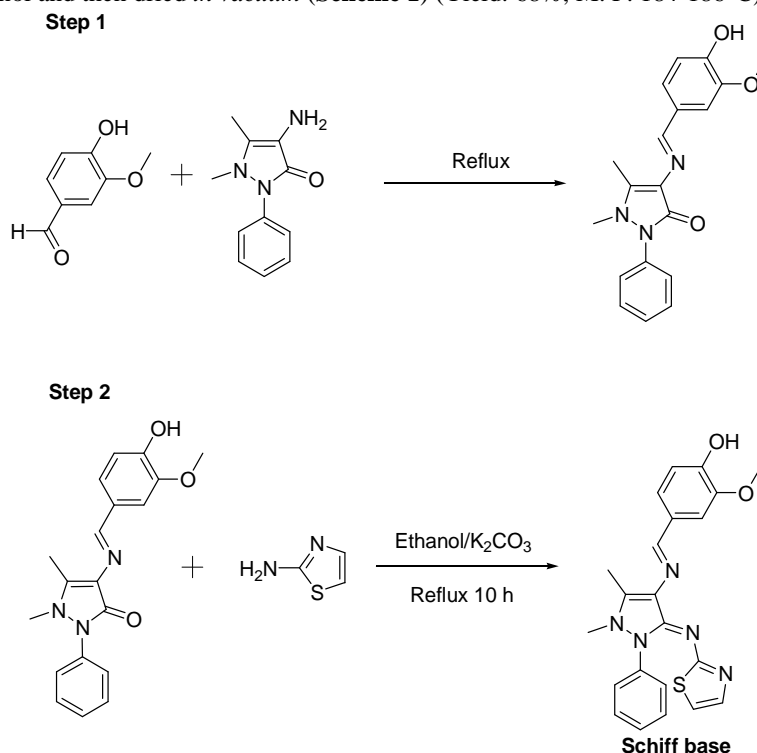
4-Aminoantipyridine and 4-hydroxy-3-methoxybenzaldehyde were obtained from Sigma. 2-aminothiazole was purchased from SD Finechem Ltd. Metal chlorides were purchased from Merck. All chemicals used were of AR grade. Molar conductivity was determined using Systronic Conductivity Bridge with a dip type cell using freshly prepared 10^{-3} M solutions in DMSO at RT. The IR spectra were recorded in KBr pellet on a Perkin-Elmer 783 spectrometer in the range $4000\text{-}400\text{ cm}^{-1}$. UV-Visible spectra of the complexes were recorded on Perkin Elmer Lambda EZ201 spectrophotometer in DMSO solution. $^1\text{H-NMR}$ spectra were recorded on a Bruker 300 MHz instrument using CDCl_3 as a solvent and TMS as an internal standard. The RT magnetic measurements were carried out using Guoy balance and the diamagnetic corrections were made using Pascal's constant. FAB-MS spectra were recorded with a VGZABHS spectrometer at RT in a 3-nitrobenzylalcohol matrix. Cyclic Voltammetry studies were performed on a CHI 760C electrochemical analyzer in single compartmental cells at RT using tetrabutylammonium perchlorate (TBAP) as a supporting electrolyte. X-band EPR spectra of the copper complexes were recorded in DMSO at RT and LNT at Sophisticated Analytical Instrument Facility (SAIF), IIT, Mumbai.

The Schiff base ligand was synthesized by two approaches as given below.

2.2. Synthesis of Schiff base ligand

Method 1

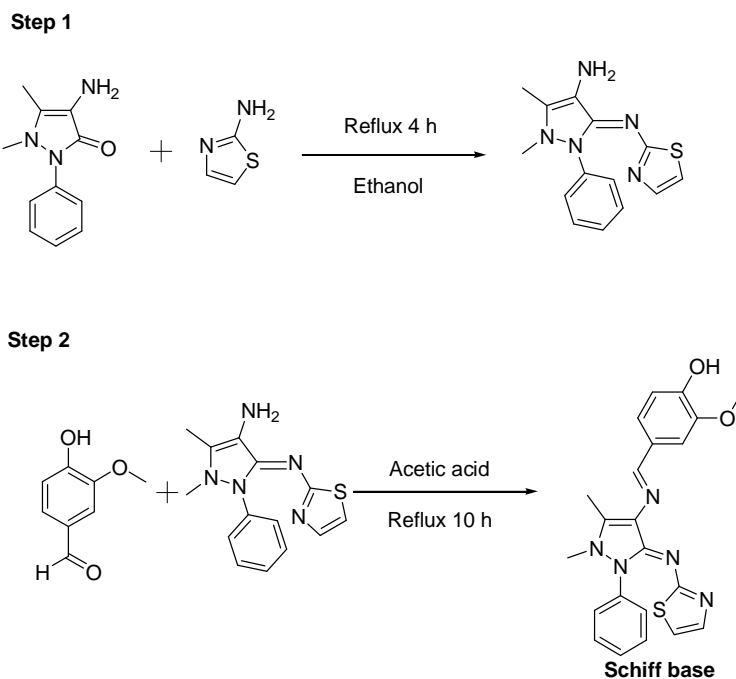
4-hydroxy-3-methoxybenzylidene-4-aminoantipyridine was synthesized by the condensation of 4-hydroxy-3-methoxybenzaldehyde and 4-aminoantipyridine as reported earlier [13]. 4-hydroxy-3-methoxybenzylidene-4-aminoantipyridine (0.01 mol) and 2-aminothiazole (0.01 mol) were taken in ethanol. To this mixture, 1 g of anhydrous potassium carbonate was added and then refluxed for 10 hours. The resulting solution was concentrated on a water bath and allowed to cool at 0°C for ~ 24 h. The solid product formed was separated by filtration and washed thoroughly with ethanol and then dried *in vacuo* (Scheme 1) (Yield: 68%, M. P. $184\text{-}186^\circ\text{C}$).



Scheme 1. Synthesis of Schiff base method 1

Method 2

4-aminoantipyrine-2-aminothiazole was synthesized as reported earlier [16]. Vanillin (0.01 mol) and 4-aminoantipyrine-2-aminothiazole (0.01 mol) were dissolved in hot ethanol. A few drops of acetic acid were added and the solution was refluxed for 10 h with continuous stirring. The Schiff base product formed was filtered and recrystallized from ethanol (**Scheme 2**) (Yield: 60%). From these two methods the first one gave a better yield of the Schiff base ligand.



Scheme 2. Synthesis of Schiff base by method 2

2.3. Synthesis of metal complexes

A solution of metal(II) chloride in ethanol (2 mmol) was stirred with an ethanolic solution of the Schiff base (2 mmol), for 2 h on a magnetic stirrer at room temperature. Then the solution was concentrated to one third of the volume on a water bath. The solid product so formed was separated and washed thoroughly with hot ethanol and dried *in vacuo*.

2.4. In silico studies on DNA and metal complexes

The interaction of the metal complexes with DNA was also studied by molecular modeling with special reference to docking. The crystal structure of the complex of netropsin with B-DNA dodecamer d(CGCGAATTCGCG)₂ (NDB code GDLB05) was downloaded from Protein Data Bank (PDB). Initially, the crystallographic water molecules were removed from the DNA. On the basis of literature evidences [14-16], we have selected the DNA sequence and it was subjected to DNA sequence to structure web server [17] for generating the three-dimensional model of DNA based on experimental fiber-diffraction studies [18]. The structure of the metal complexes was drawn using ChemDraw Ultra10.0 program and three-dimensional structure of metal complexes was prepared by using Discovery studio 3.1 [19]. The DNA-metal complex interaction was studied using Patch dock web server [20]. The PyMol stand-alone program [21] was used to visualize the interaction between DNA structure and metal complexes. HBAT [22], the hydrogen bond analysis tool was used to analyze the strong and weak hydrogen bonds present between DNA and metal complexes. In this program, the standard hydrogen bond distance (H...A) and angle (X-H...A) was set as 2.8 Å and 90°, respectively.

2.5. Antibacterial activity

The antimicrobial activity of Schiff bases and their metal complexes against human pathogenic bacteria was studied by agar *well-diffusion* method. Fresh bacterial cultures of gram negative bacteria namely *Pseudomonas aeruginosa*, *Escherichia coli*, *Proteus vulgaris* and gram positive bacteria *Bacillus subtilis* (MTCC 41) and *Staphylococcus aureus* (MTCC 96) were used for the antibacterial test. The colonies of the stains were inoculated to Brain Heart Infusion broth and incubated at 37°C for 24 h in orbit shaker at 200 rpm. Turbidity was adjusted with sterile broth to

correspond to the 0.5 McFarland standards before swabbing; standard inoculum of the microorganism was of 1.5×10^6 colony forming units (CFU mL⁻¹) diluted to 1:100 and given suspension of turbidity equal to a McFarland standard 0.5. The turbidity was adjusted to match a McFarland 0.5 mL of 1.175% w/v (0.048 M) BaCl₂.H₂O to 99.5 mL of 1% w/v (0.36) sulphuric acid. The antimicrobial properties of test compounds were determined by the *well-diffusion* method [23]. Standard antibiotic Tetracycline was used as reference. Organisms (24 h old culture) were swabbed on the Mueller Hinton Agar (MHA) plates with sterilized cotton swab sticks. Wells (9 mm diameter) were cut using a sterile cork borer. Stock solutions of all compounds (25) were diluted with dimethyl sulfoxide. The stock solutions were prepared for 3 mg of Compound/2 mL of DMSO concentration. From the stock solution, different diluted measurements such as 20 μ L, 40 μ L 60 μ L (20 μ L diluted sample contains 30 μ g of the test compound) were immediately dispensed into agar wells of culture inoculated plates (MHA) using sterilized microchips. The plates were incubated at 37°C overnight. The antibacterial activity was measured as the diameter of the inhibition zone including the diameter of the well.

RESULTS AND DISCUSSION

The synthesized compounds are colored, non-hygroscopic, insoluble in water, soluble in hot ethanol, DMSO and DMF. The coordination of the metal to the tridentate ligand is through the two N atoms of azomethine group and one N atom of thiazole ring. Composition and identity of the complexes were deduced from elemental analysis (Table 1) and spectroscopic studies (IR, UV-Vis, ¹H-NMR, EPR and Mass), magnetic and electrochemical studies. The results of the elemental analyses of the complexes are in good agreement with those required by the proposed formulae. In all cases the complexes isolated are found to have the general formula [ML₂] Cl₂ where M = Cu(II), Co(II), Ni(II) and Zn(II). The conductance measurements show that the complexes are electrolytes [24] (82-96 $\Omega^{-1} \text{cm}^2 \text{mol}^{-1}$) and the mass spectra determinations indicate their monomeric nature.

Table 1 Color, reaction yield and elemental analysis of the ligand and its metal complexes

Compound	Empirical Formula	Yield (%)	Color	Found (Calculated) (%)				Formula weight	χ_M $\Omega^{-1} \text{cm}^2 \text{mol}^{-1}$	μ_{eff} (B.M.)
				M	C	H	N			
L	C ₂₂ H ₂₁ N ₅ O ₂ S	68	Yellow	-	62.77 (62.99)	4.71 (5.05)	15.95 (16.09)	419.4	-	-
[CuL ₂] Cl ₂	CuC ₄₄ H ₄₂ N ₁₀ O ₄ S ₂	52	Green	6.76 (7.04)	57.89 (58.55)	4.34 (4.69)	15.02 (15.52)	902.5	82	1.86
[CoL ₂] Cl ₂	CoC ₄₄ H ₄₂ N ₁₀ O ₄ S ₂	54	Brown	6.27 (6.56)	58.45 (58.85)	4.34 (4.71)	15.12 (15.60)	897.9	88	4.42
[NiL ₂] Cl ₂	NiC ₄₄ H ₄₂ N ₁₀ O ₄ S ₂	63	Green	6.14 (6.54)	58.35 (58.87)	4.34 (4.72)	15.07 (15.60)	897.6	93	2.94
[ZnL ₂] Cl ₂	ZnC ₄₄ H ₄₂ N ₁₀ O ₄ S ₂	60	Yellow	7.19 (7.23)	58.15 (58.43)	4.45 (4.68)	15.38 (15.49)	904.3	96	Diamagnetic

Table 2 The IR spectral data of Schiff base and its metal complexes (cm⁻¹)

Compound	$\nu(\text{OH})$	$\nu(\text{CH=N})$ of thiazole	$\nu(\text{C-S})$ of thiazole	$\nu(\text{C=N})$	$\nu(\text{M-N})$	$\nu(\text{M-O})$
Schiff base (L)	3139	1560	835	1595, 1660	-	-
[CuL ₂] Cl ₂	3185	1537	838	1572, 1622	425	535
[CoL ₂] Cl ₂	3128	1520	842	1578, 1615	464	555
[NiL ₂] Cl ₂	3174	1532	856	1580, 1627	438	533
[ZnL ₂] Cl ₂	3156	1540	830	1579, 1620	482	518

3.1. Mass Spectra

The ESI mass spectra of the Schiff base ligand (L) and its copper complex [CuL₂] Cl₂ recorded at RT were used to compare their stoichiometry. The Schiff base showed the molecular ion peak at *m/z* 419. The molecular ion peak for the copper complex, observed at *m/z* 902 confirms the stoichiometry of metal complexes as [ML₂] Cl₂ type. It is also supported by the mass spectra of other complexes. Mass spectra of Schiff base and its copper complex are given in Figs. 1 and 2. Microanalytical data are also in close agreement with the values calculated from molecular formula assigned to these complexes.

Table 3 Electronic spectral data of Schiff base and its complexes

Compound	Absorption nm (cm ⁻¹)	Band assignments	Geometry
Schiff base (L)	298 (33,557)	INCT	-
[CuL ₂] Cl ₂	295 (33,298) 676 (14,792)	INCT ² E _g → ² T _{2g} transition	Octahedral
[CoL ₂] Cl ₂	296 (33,783) 420 (23,809) 596 (16,778) 685 (14,498)	INCT ⁴ T _{1g} (F) → ⁴ T _{1g} (P) transition ⁴ T _{1g} (F) → ⁴ A _{2g} (F) transition ⁴ T _{1g} (F) → ⁴ T _{2g} (F) transition	Octahedral
[NiL ₂] Cl ₂	310 (32,258) 418 (23,923) 605 (16,528) 710 (14,084)	INCT ³ A _{2g} (F) → ³ T _{1g} (P) transition ³ A _{2g} (F) → ³ T _{1g} (F) transition ³ A _{2g} (F) → ³ T _{2g} (F) transition	Octahedral

Table 4 Shape complementarity score of DNA-Metal Complex

S. No	Compound	Shape-Complementarity Score
1.	DNA – [CoL ₂] Cl ₂	4718
2.	DNA – [CuL ₂] Cl ₂	4666
3.	DNA – [NiL ₂] Cl ₂	4578
4.	DNA – [ZnL ₂] Cl ₂	4456

Table 5 Inter-molecular hydrogen bonds present in DNA-cobalt complex

Type	Donor	Donor Atom	Acceptor	Acceptor Atom	d (H...A) (Å)	D (X...A) (Å)	q (X-H...A) (°)
C-H...N	Cytosine	C4	[CoL ₂] Cl ₂	N7	2.783	3.627	134.0
C-H...N	Cytosine	C4	[CoL ₂] Cl ₂	N16	2.700	3.651	145.5
C-H...N	Cytosine	C4	[CoL ₂] Cl ₂	N29	2.456	3.139	119.4
C-H...O	Guanine	C4	[CoL ₂] Cl ₂	O25	2.749	3.445	121.3
C-H...O	[CoL ₂] Cl ₂	C19	Guanine	O4	2.522	3.270	125.5
C-H...O	[CoL ₂] Cl ₂	C22	Adenine	O4	2.085	2.539	101.9
C-H...O	[CoL ₂] Cl ₂	C22	Adenine	O3	2.902	3.580	120.9
C-H...O	Adenine	C4	[CoL ₂] Cl ₂	O24	0.966	1.805	112.5
O-H...O	[CoL ₂] Cl ₂	O24	Adenine	O5	2.860	3.410	117
O-H...O	Guanine	O4	[CoL ₂] Cl ₂	O25	2.065	3.074	172.5
C-H...O	[CoL ₂] Cl ₂	C26	Guanine	O4	1.014	2.013	146
C-H...O	[CoL ₂] Cl ₂	C26	Guanine	O3	2.705	3.295	113.5
C-H...O	[CoL ₂] Cl ₂	C30	Thymine	O4	2.823	3.455	116.8
C-H...O	[CoL ₂] Cl ₂	C30	Thymine	O2	2.397	3.472	168.3
C-H...O	[CoL ₂] Cl ₂	C31	Thymine	O2	2.598	3.676	170.4
C-H...O	[CoL ₂] Cl ₂	C31	Cytosine	O4	1.988	2.327	93.64
C-H...O	[CoL ₂] Cl ₂	C47	Thymine	O3	2.534	3.545	155.4
C-H...O	[CoL ₂] Cl ₂	C54	Thymine	O3	1.885	2.480	109.9
C-H...O	[CoL ₂] Cl ₂	C54	Thymine	O1P	2.058	2.864	128.1
C-H...O	[CoL ₂] Cl ₂	C54	Thymine	O2P	1.951	2.590	113.7
C-H...O	[CoL ₂] Cl ₂	C59	Guanine	O2P	2.169	2.551	97.79
C-H...O	[CoL ₂] Cl ₂	C59	Guanine	O2P	2.218	2.551	95.03
C-H...O	[CoL ₂] Cl ₂	C59	Guanine	O5	2.107	2.767	116.7

3.2. Infrared Spectra

The IR spectral information of the Schiff base and its complexes are given in **Table 2**. The IR spectrum of the ligand shows a broad band in the region 3100-3200 cm⁻¹, assignable to ν_(OH) group of vanillin. The appearance of this peak in all the spectra of the complexes suggest that the -OH group does not get involved in the complexation. The spectrum of the ligand shows two different ν_(C=N) bands at 1595 and 1660 cm⁻¹, which are shifted to lower frequencies in the spectra of all the complexes (1570-1630 cm⁻¹) indicating the involvement of -C=N nitrogen in coordination to the metal ion. Also the ligand shows a band at 1560 cm⁻¹ which is attributed to ν_(CH=N) of the thiazole ring and ν_(C=C) at 1482 cm⁻¹. The stretching vibration appears at 835 cm⁻¹ is due to ν_(C-S) of the thiazole ring [25]. A shift in the band ν_(CH=N) of the thiazole ring (1520-1540 cm⁻¹) in complexes indicates the coordination via thiazole nitrogen (N → M). In all the complexes the ν_(C-S) remains unchanged indicating that the sulphur is not involved in the coordination. IR spectra of complexes show new bands at 425-482 cm⁻¹ and 518-555 cm⁻¹ assigned to ν_(M-N) and ν_(M-O) modes respectively.

Table 6 Inter-molecular hydrogen bonds present in DNA-copper complex

Type	Donor	Donor Atom	Acceptor	Acceptor Atom	d (H...A) (Å)	D (X...A) (Å)	q (X-H...A) (°)
C-H...O	Adenine	C4	[CuL ₂] Cl ₂	O52	2.223	3.194	147.1
C-H...S	Thymine	C4	[CuL ₂] Cl ₂	S11	1.979	2.665	117.5
C-H...Cl	Guanine	C4	[CuL ₂] Cl ₂	Cl62	2.096	2.385	91.29
C-H...Cl	Guanine	C3	[CuL ₂] Cl ₂	Cl62	2.874	3.097	91.25
C-H...O	[CuL ₂] Cl ₂	C2	Thymine	O4	2.764	3.647	138.8
C-H...O	[CuL ₂] Cl ₂	C2	Thymine	O2	2.915	3.829	142.5
C-H...O	[CuL ₂] Cl ₂	C3	Thymine	O4	2.194	3.863	117.8
C-H...O	[CuL ₂] Cl ₂	C10	Thymine	O1P	2.928	3.684	127.1
O-H...O	[CuL ₂] Cl ₂	O24	Adenine	O5	2.860	3.410	117
O-H...O	Guanine	O4	[CuL ₂] Cl ₂	O25	2.065	3.074	172.5
C-H...O	[CuL ₂] Cl ₂	C30	Thymine	O3	2.026	2.702	117
C-H...O	[CuL ₂] Cl ₂	C30	Cytosine	O1P	2.648	3.122	105.5
C-H...O	[CuL ₂] Cl ₂	C30	Cytosine	O5	2.759	3.805	160.7
C-H...O	[CuL ₂] Cl ₂	C30	Cytosine	O1P	2.645	3.122	105.6
C-H...O	[CuL ₂] Cl ₂	C54	Cytosine	O4	2.061	3.043	148.2

Table 7 Inter-molecular hydrogen bonds present in DNA-nickel complex

Type	Donor	Donor Atom	Acceptor	Acceptor Atom	d (H...A) (Å)	D (X...A) (Å)	q (X-H...A) (°)
C-H...N	[NiL ₂] Cl ₂	C12	Adenine	N6	2.252	3.018	126.3
C-H...O	[NiL ₂] Cl ₂	C12	Thymine	O4	1.788	2.726	142.7
C-H...N	[NiL ₂] Cl ₂	C13	Adenine	N6	2.580	3.150	111.6
C-H...N	[NiL ₂] Cl ₂	C13	Adenine	N6	2.195	3.031	131.7
C-H...O	[NiL ₂] Cl ₂	C38	Adenine	O2P	2.356	2.864	106.9
C-H...O	[NiL ₂] Cl ₂	C39	Adenine	O2P	2.957	3.162	90.74
C-H...N	[NiL ₂] Cl ₂	C40	Adenine	N7	2.805	3.247	104.3
C-H...O	[NiL ₂] Cl ₂	C54	Adenine	O5	2.906	3.387	106.8
C-H...O	[NiL ₂] Cl ₂	C54	Adenine	O3	2.707	3.565	135.1
C-H...O	[NiL ₂] Cl ₂	C54	Adenine	O1P	2.753	3.746	151
C-H...O	[NiL ₂] Cl ₂	C54	Adenine	O2P	0.380	1.280	111.4
C-H...O	[NiL ₂] Cl ₂	C54	Adenine	O5	2.888	3.387	107.9
C-H...N	[NiL ₂] Cl ₂	C55	Adenine	N7	2.700	3.505	130.3
C-H...N	[NiL ₂] Cl ₂	C55	Adenine	N6	2.197	3.185	149.4
C-H...O	[NiL ₂] Cl ₂	C56	Thymine	O4	2.592	3.679	174.4
C-H...O	[NiL ₂] Cl ₂	C57	Adenine	O2P	2.956	3.434	105.7
C-H...N	[NiL ₂] Cl ₂	C57	Adenine	N7	2.973	3.789	129.8
C-H...O	[NiL ₂] Cl ₂	C59	Adenine	O2P	2.124	2.924	128.6

Table 8 Inter-molecular hydrogen bonds present in DNA-zinc complex

Type	Donor	Donor Atom	Acceptor	Acceptor Atom	d (H...A) (Å)	D (X...A) (Å)	q (X-H...A) (°)
C-H...O	[ZnL ₂] Cl ₂	C4	Adenine	O1P	2.620	3.381	126.8
C-H...N	[ZnL ₂] Cl ₂	C22	Adenine	N7	2.841	3.804	148.4
C-H...N	[ZnL ₂] Cl ₂	C22	Adenine	N6	2.732	3.478	125.8
C-H...O	[ZnL ₂] Cl ₂	C22	Thymine	O4	2.112	2.566	102
C-H...O	[ZnL ₂] Cl ₂	C6	[ZnL ₂] Cl ₂	O24	0.967	1.901	146.6
O-H...N	[ZnL ₂] Cl ₂	O24	Adenine	N1	2.213	3.087	149.7
O-H...N	[ZnL ₂] Cl ₂	O24	Adenine	N6	0.513	1.134	94.99
C-H...N	[ZnL ₂] Cl ₂	C26	Adenine	N7	1.774	2.380	110
C-H...N	[ZnL ₂] Cl ₂	C26	Adenine	N9	2.676	3.347	119.2
C-H...O	[ZnL ₂] Cl ₂	C37	Guanine	O5	2.919	3.389	106.5
C-H...O	[ZnL ₂] Cl ₂	C38	Cytosine	O3	2.349	3.408	166.3
C-H...O	[ZnL ₂] Cl ₂	C38	Guanine	O2P	1.142	1.590	91.31
C-H...O	[ZnL ₂] Cl ₂	C38	Guanine	O5	2.804	3.334	110
C-H...O	[ZnL ₂] Cl ₂	C39	Cytosine	O5	2.952	3.949	153.4
C-H...O	[ZnL ₂] Cl ₂	C54	Adenine	O5	2.941	3.518	113.1
C-H...O	Adenine	C2	[ZnL ₂] Cl ₂	O2P	2.162	2.691	100.8
C-H...O	Adenine	C2	[ZnL ₂] Cl ₂	O53	2.066	3.059	133.3
C-H...O	[ZnL ₂] Cl ₂	C54	Adenine	O3	1.781	2.798	153.2

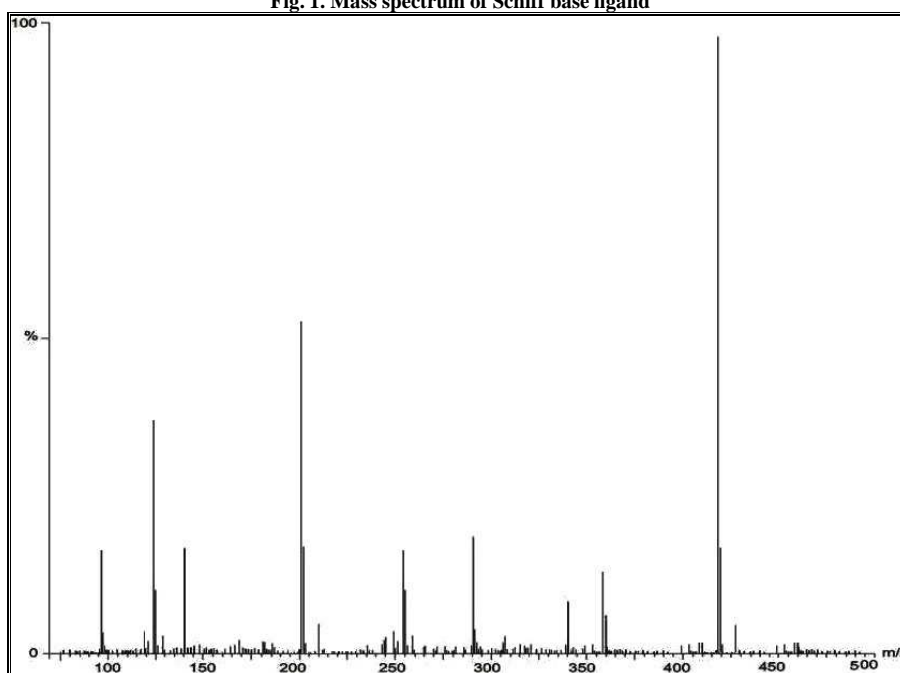
Table 9 Statistics of inter-molecular hydrogen bonds present between DNA and metal complex

Metal Complex	N-H...O	O-H...O	N-H...N	N-O-H...N	N-C-H...O	O-C-H...N	N-H...S	S-O-H...S	S-C-H...S	S-C-H...Cl
DNA – [CoL ₂] Cl ₂	0	2	0	0	18	3	0	0	0	0
DNA – [CuL ₂] Cl ₂	0	2	0	0	10	0	0	0	1	2
DNA – [NiL ₂] Cl ₂	0	0	0	0	11	7	0	0	0	0
DNA – [ZnL ₂] Cl ₂	0	0	0	2	12	4	0	0	0	0

Table 10 Antimicrobial activity data for Schiff base and its complexes

Compound	<i>B. subtilis</i>			<i>S. aureus</i>			<i>P. vulgaris</i>			<i>P. aeruginosa</i>		
	20µL	40µL	60µL	20µL	40µL	60µL	20µL	40µL	60µL	20µL	40µL	60µL
L	-	10	12	10	12	16	-	9	11	-	-	12
[CuL ₂] Cl ₂	-	12	14	10	12	18	-	11	13	-	10	14
[CoL ₂] Cl ₂	10	12	13	10	11	14	-	11	14	9	12	14
[NiL ₂] Cl ₂	-	11	14	9	10	14	-	11	12	8	13	14
[ZnL ₂] Cl ₂	12	13	15	14	15	18	-	10	12	-	12	14

Fig. 1. Mass spectrum of Schiff base ligand



3.3. ¹H-NMR spectra

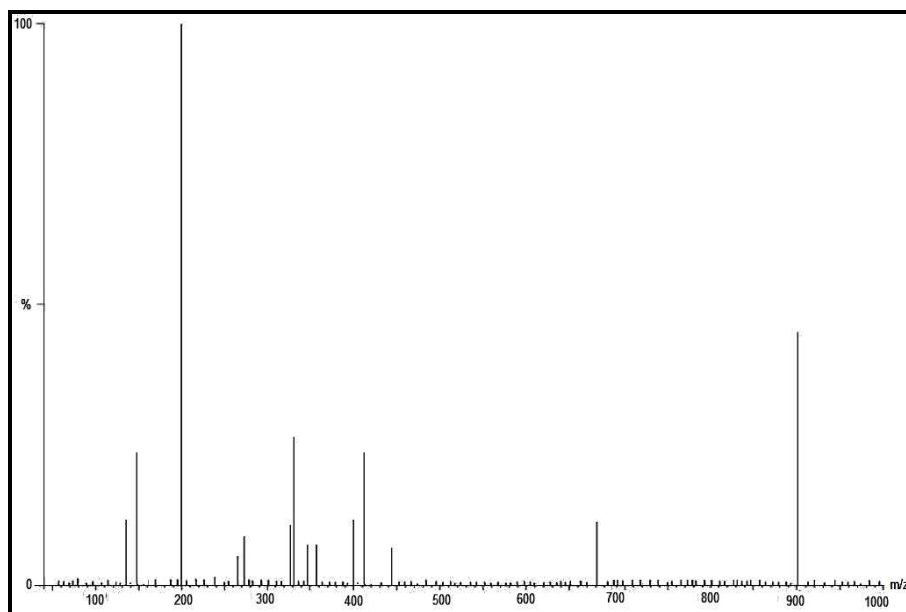
¹H NMR spectra of the Schiff base ligand and its zinc complex were recorded at RT in CDCl₃. Schiff base ligand (L) exhibited the following signals: aromatic protons at 6.84-7.38 δ (8H, m), -CH=N at 9.78 δ (1H, s), -N-CH₃ at 3.14 δ (3H, s), C-CH₃ at 2.48 δ (3H, s), -O-CH₃ at 3.96 δ (3H, s), -OH proton at 6.13 δ (1H, s) and S-CH=CH- of thiazole ring at 7.76 δ (1H, d). Thiazole proton of free ligand at 7.94 δ (1H, d) also showed a downfield shift in the complex providing an evidence of coordination of thiazole nitrogen to the metal. The azomethine proton signals in the spectra of zinc complex were moved to downfield compared to the ligand, suggesting deshielding of azomethine group due to coordination with metal atom. There is no significant change in all other signals of the ligand. ¹H-NMR spectra of Schiff base ligand is given in **Fig. 3**.

3.4. Electronic spectra

The electronic absorption spectra of the Schiff base ligand and its complexes were recorded in DMSO solution and the spectral data are furnished in **Table 3**. The electronic spectra can often give dependable information about the ligand arrangements in the transition metal complexes. The electronic spectrum of the copper complex exhibits two bands, which are assigned as an intraligand charge-transfer band (33,298 cm⁻¹) and a *d-d* band (14,792 cm⁻¹) which is due to ²E_g → ²T_{2g} transition. This *d-d* band strongly favors distorted octahedral geometry around the metal ion. It is also supported by the magnetic susceptibility value (1.86 B.M). The cobalt complex showed four absorption bands

at 33,783, 23,809, 16,778, and 14,498 cm^{-1} , which are assigned as charge transfer, ${}^4\text{T}_{1g}(\text{F}) \rightarrow {}^4\text{T}_{2g}(\text{P})$, ${}^4\text{T}_{1g}(\text{F}) \rightarrow {}^4\text{A}_{2g}(\text{F})$ and ${}^4\text{T}_{1g}(\text{F}) \rightarrow {}^4\text{T}_{2g}(\text{F})$ transitions, respectively. The band at 14,498 cm^{-1} confirmed the octahedral geometry, which is also supported by its magnetic susceptibility value (4.42 B.M). The nickel complex revealed three $d-d$ bands at 14,084, 16,528, and 23,923 cm^{-1} which are assigned to ${}^3\text{A}_{2g}(\text{F}) \rightarrow {}^3\text{T}_{2g}(\text{F})$, ${}^3\text{A}_{2g}(\text{F}) \rightarrow {}^3\text{T}_{1g}(\text{F})$ and ${}^3\text{A}_{2g}(\text{F}) \rightarrow {}^3\text{T}_{1g}(\text{P})$ transitions, respectively, being characteristic of an octahedral geometry supported by its magnetic susceptibility value (2.94 B.M).

Fig. 2. Mass spectrum of copper complex



3.5. Redox study

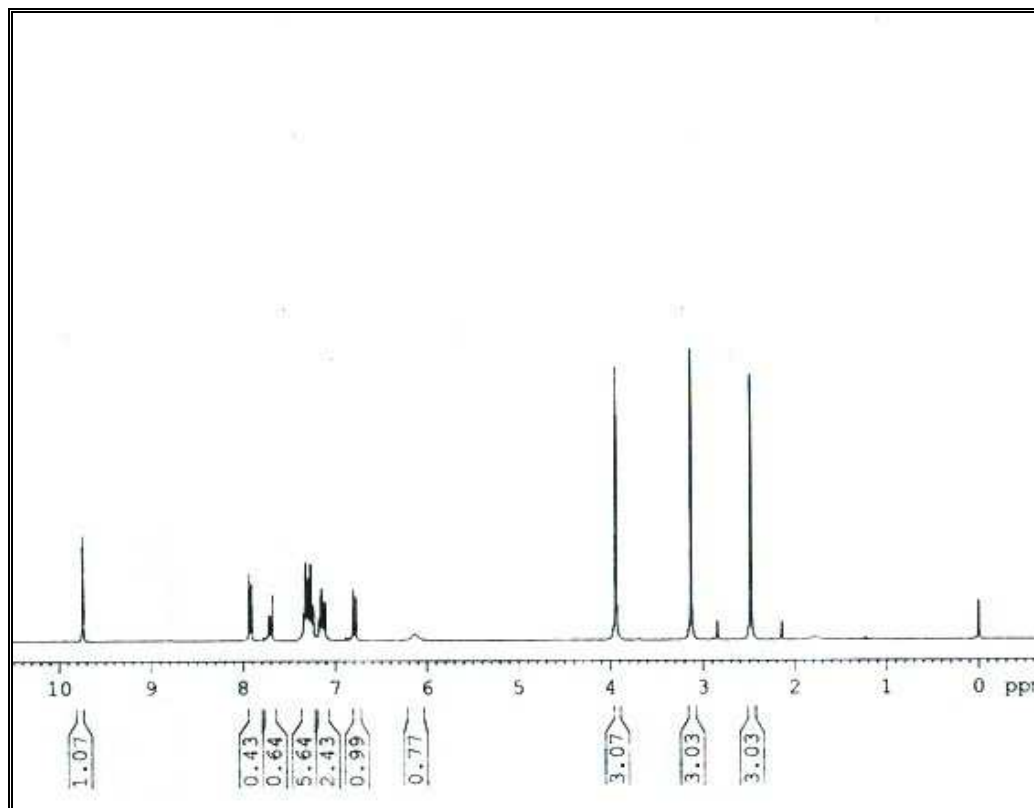
The cyclic voltammogram of the copper complex in DMSO (from 0.8 to -1.0 V potential range) shows a well defined redox process corresponding to the formation of the Cu(II)/Cu(III) couple at $E_{\text{pa}} = 0.358$ V and the associated anodic peak at $E_{\text{pc}} = 0.252$ V (Fig. 4). This couple is found to be reversible with $\Delta E_p = 0.106$ V and the ratio of anodic to cathodic peak currents corresponds to a simple one-electron process. Copper complex also shows a reversible peak in the negative region characteristic of the Cu(II)/Cu(I) couple at $E_{\text{pa}} = -0.364$ V with the associated anodic peak at $E_{\text{pc}} = -0.508$ V for Cu(I)/Cu(II) oxidation.

3.6. Electron paramagnetic resonance spectra

The EPR spectrum of copper complex gives important information in studying the metal ion environment. The EPR spectra were recorded in DMSO at RT and LNT (Fig. 5 and 6). The spectrum of the copper complex at RT shows one intense absorption band in the high field and is isotropic due to the tumbling motion of the molecules. However, this complex at LNT shows well resolved peaks at low field region. The copper complex displays the g_{\parallel} value of 2.268 and g_{\perp} value of 2.069. These values show that Cu(II) complex lies predominantly in the $d_{x^2-y^2}$ orbital, as was obvious from the value of the exchange interaction term G , estimated from the expression: $G = (g_{\parallel} - 2.00277)/(g_{\perp} - 2.00277)$.

If $G > 4.0$, the local tetragonal axes are aligned parallel or only slightly misaligned. If $G < 4.0$, significant exchange coupling is present and the misalignment is significant. The observed value for the exchange interaction parameter for the copper complex $G > 4.0$ suggests that the local tetragonal axes are aligned parallel or slightly misalignment and the unpaired electron is present in the $d_{x^2-y^2}$ orbital. This result also explains that the exchange coupling effects are not operative in the present complex [26].

Based on the above spectral and analytical data, the proposed structure of the Cu(II), Co(II), Ni(II) and Zn(II) complexes is given in Fig. 7.

Fig. 3. ¹H-NMR spectrum of Schiff base ligand

3.7. *In silico* DNA-metal complex interaction

The Patch dock web server was used to study the interaction between DNA and metal complexes. One hundred docking conformations were generated for each metal complex with the DNA molecule. The best docking solution was inferred by highest value of shape complementarity score (**Table 4**). The shape-complementarity score of four complexes was computed using Patch dock web server. From the molecular docking results (**Fig. S8**), the best solution was selected and it was processed into Hydrogen Bond Analysis Tool (HBAT) for computing the possible inter-molecular hydrogen bonds present between DNA and metal complexes. The results showed that inter-molecular C-H...O hydrogen bond played a crucial role for the stability of all metal complexes with DNA. The information of inter-molecular C-H...O, C-H...N, O-H...O, O-H...N, C-H...Cl and C-H...S interactions were given in **Tables 5-8**. Cobalt, nickel and zinc complexes contain inter-molecular C-H...O and C-H...N interactions and copper complex having C-H...O, O-H...O, C-H...S and C-H...Cl interactions. However, all the four complexes did not contain other inter-molecular hydrogen bonds such as N-H...O, N-H...N, N-H...S, O-H...S, C-H... π , N-H... π and O-H... π . **Fig. 9** and **Table 9** explain the statistics of various possible inter-molecular hydrogen bonds present between DNA and metal complexes.

Patch dock and HBAT analysis results suggest that cobalt and copper complexes are bound to the “Minor groove” and nickel and zinc complexes are bound to the “Major groove” portion of DNA through hydrogen bonds and hence they are called “Minor groove and Major groove binders” respectively.

3.7. Antimicrobial study

The *in vitro* biological screening effects of the compounds were tested against gram positive bacteria such as *Staphylococcus aureus*, *Bacillus subtilis* and gram negative such as *Pseudomonas aeruginosa* and *Proteus vulgaris* by well-diffusion method. The zone of inhibition (diameter in mm) value of the compounds against the growth microorganisms are summarized in **Table 10**. A comparison of the zone of inhibition value of ligand and its complexes shows that the metal complexes exhibited higher activity than the ligand and control. Such increased

activity of the complexes can be explained based on the Overtone's concept [27] and the Tweedy chelation theory [28].

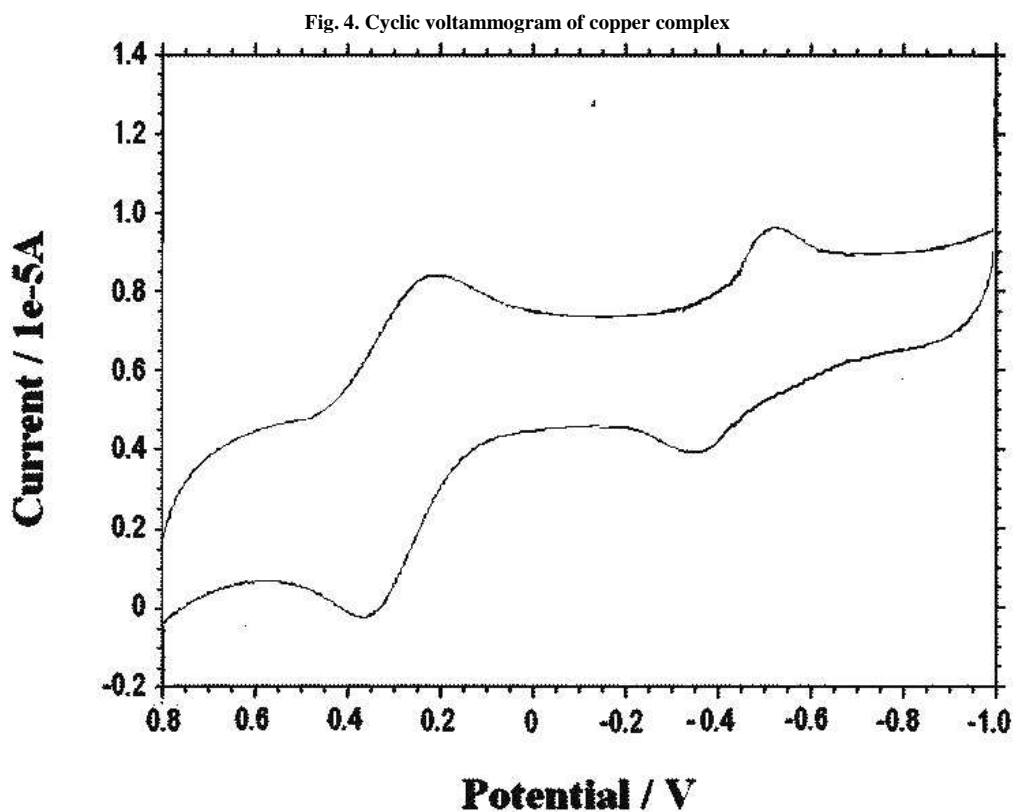


Fig. 5. ESR spectra of copper complex at room temperature

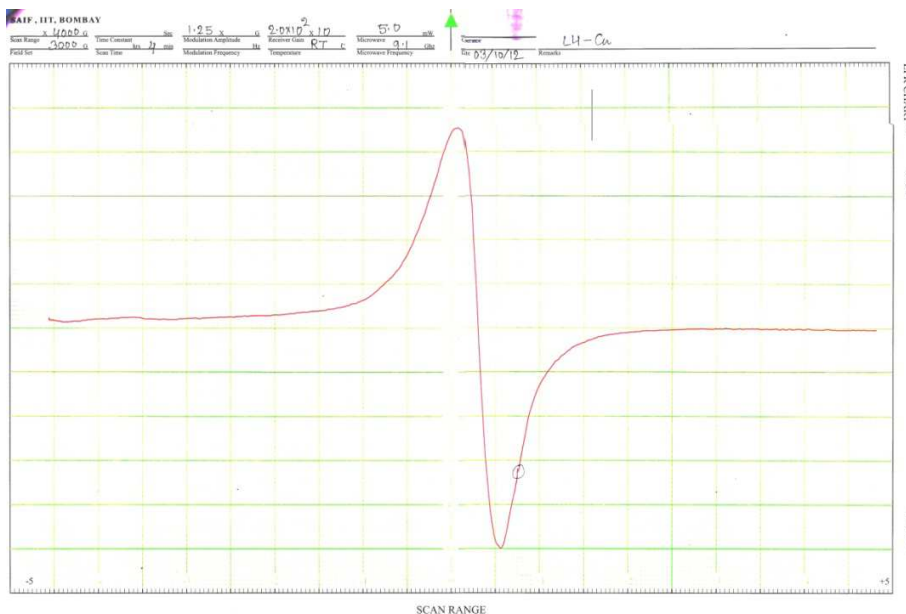


Fig. 6. ESR spectra of copper complex at liquid nitrogen temperature

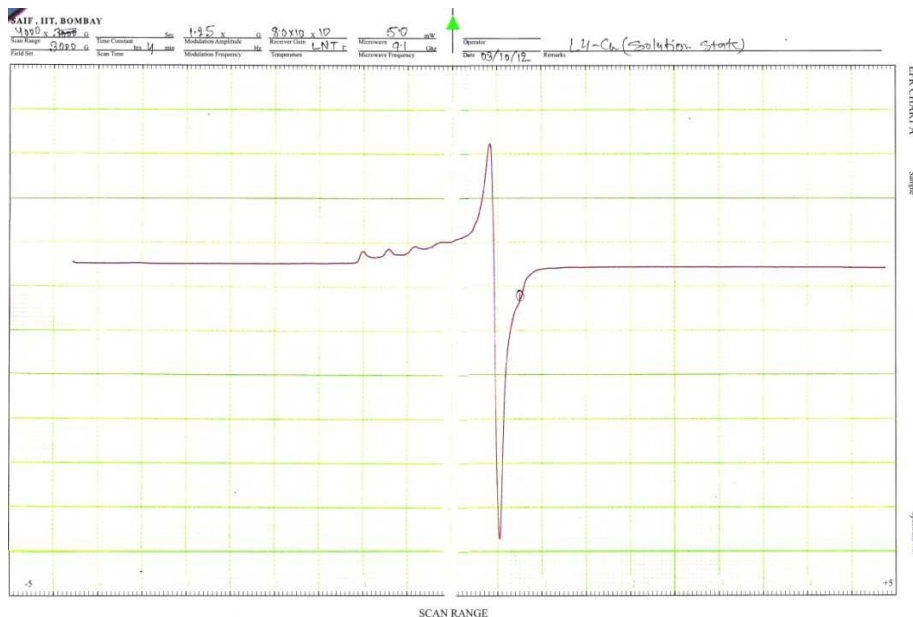


Fig. 7. Octahedral geometry of metal complexes where M = (Cu(II), Co(II), Ni(II) and Zn(II))

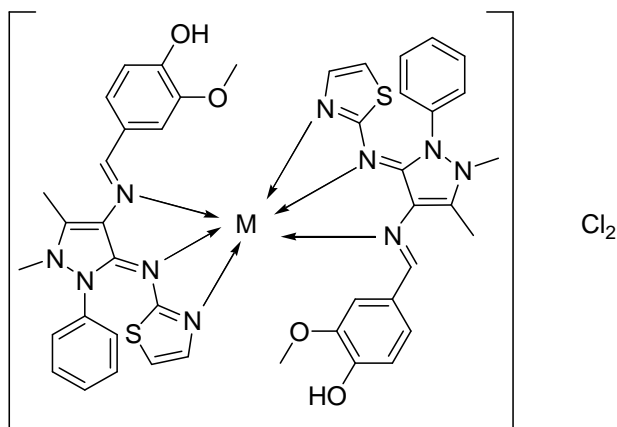


Fig. 8. Molecular docking results of DNA–metal complex interaction (a) DNA–[CoL₂] Cl₂, (b) DNA–[CuL₂] Cl₂, (c) DNA–[NiL₂] Cl₂ and (d) DNA–[ZnL₂] Cl₂ complex. [Color codes: Ligand: Yellow, Representation: Stick, Display: PyMol]

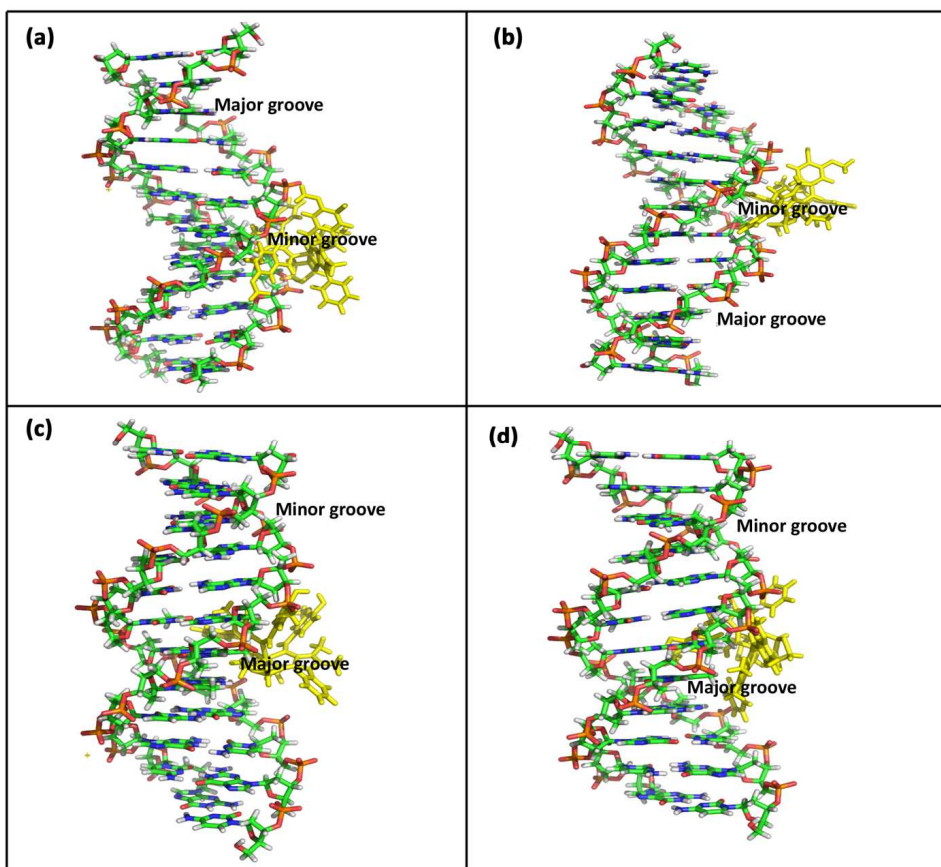
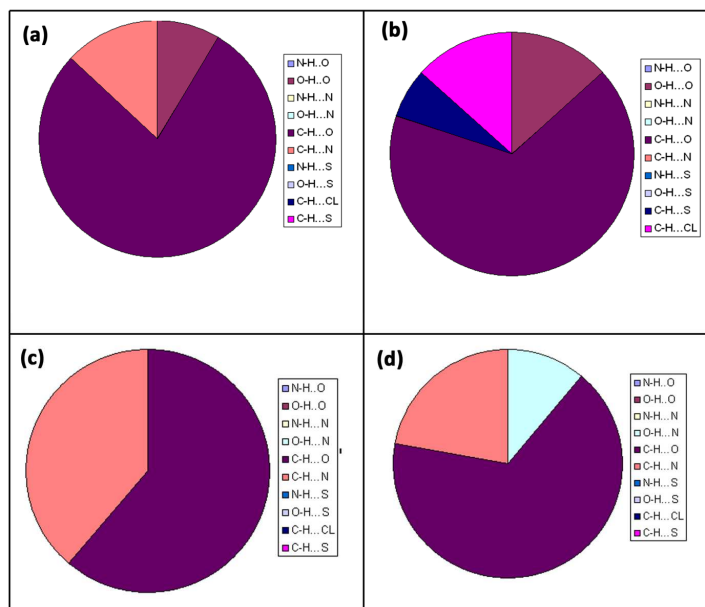


Fig. 9. Statistics of various possible inter-molecular hydrogen bonds present between DNA and metal complex a) cobalt b) copper c) nickel and d) zinc complex



CONCLUSION

The coordination chemistry of the Schiff base ligand obtained from the reaction of 4-aminoantipyrine, 4-hydroxy-3-methoxybenzaldehyde and 2-aminothiazole is described. Cu(II), Co(II), Ni(II), and Zn(II) complexes of the ligand have been characterized by spectral and analytical data. The IR, electronic transition and ESR data lead to the conclusion that the Cu(II) complex assumes a distorted octahedral geometry and the other complexes of Co(II), Ni(II) and Zn(II) are octahedral in nature. In all the complexes, the ligand acts as a tridentate. The *in silico* DNA results reveal that cobalt and copper complexes are bound to the “Minor groove and nickel and zinc complexes are bound to the “Major groove” portion of DNA through hydrogen bonds and hence they are called “Minor groove and Major groove binders” respectively. The antibacterial screening data reveal that the complexes have higher antimicrobial activity than the free ligand.

Acknowledgements

The authors express their sincere to IIT, Bombay, India for ESR spectra. We are thankful to CDRI, Lucknow for elemental analyses.

REFERENCES

- [1] KS Prasad; L Shiva Kumar; S Chandan; B Jayalakshmi. *Spectrochim. Acta A*, **2011**, 81, 276- 282.
- [2] S Yamada. *Coord. Chem. Rev.*, **1999**, 192, 537.
- [3] K Nagashri; J Joseph; CJ Dhanraj. *Appl. Organometal. Chem.*, **2011**, 25, 704-717.
- [4] A Nori; J Kopecek. *Adv. Drug Deliv. Rev.*, **2005**, 57, 609-636.
- [5] M Shi; K Ho; A Keating; MS Shoichek. *Adv. Funct. Mater.*, **2009**, 19, 1689-1696.
- [6] G Raja; RJ Butcher; C Jayabalakrishnan. *Spectrochim. Acta A*, **2012**, 94, 210-215.
- [7] N Raman; JD Raja; A Sakthivel. *J. Chem. Sci.*, **2007**, 119, 303-310.
- [8] T Punniyamurthy; SJS Kalra; J Iqbal; *Tetrahedron Lett.* 1995: 36; 8497-8500.
- [9] JG Michael; ML Tachel; LM Susanm; HB John; LB Milton. *Bioorg. Med. Chem.*, **2004**, 12, 1029-1036.
- [10] AF Robert; *Clin. Microbiol. Rev.*, **1988**, 1, 187-217.
- [11] KY Jung; SK Kim; ZG Gao. *Bioorg. Med. Chem.*, **2004**, 12, 613-623.
- [12] M Kalanithi; D Kodimunthiri; M Rajarajan; P Tharmaraj. *Spectrochim. Acta A*, **2011**, 82, 290-298.
- [13] YK Vaghasiya; R Nair; M Soni; S Baluja; S Chanda. *J. Serb. Chem. Soc.*, **2004**, 69, 991-998.
- [14] N Raman; S Sobha; A Thamarachelvan. *Spectrochim. Acta A Mol. Biomol. Spectrosc.*, **2010**, 78, 888-898.
- [15] J Senthil Kumaran; S Priya; N Jayachandramani; S Mahalakshmi. *Journal of Chemistry*, **2013**, 10 pages.
- [16] J Senthil Kumaran; S. Priya; J. Muthukumar, N. Jayachandramani, S. Mahalakshmi. *Journal of Chemical and Pharmaceutical Research*, **2013**, 5(7), 56-69
- [17] <http://www.scfbio-iitd.res.in/software/drugdesign/bdna.jsp>
- [18] S Arnott; PJ Campbell-Smith; R Chandrasekaran; In Handbook of Biochemistry and Molecular Biology, 3rd ed. *Nucleic Acids*, Volume II, GP Fasman, Ed. Cleveland: CRC Press, **1976**, 411-422.
- [19] Accelrys Software Inc., *Discovery Studio Modeling Environment, Release 3.1*, San Diego: Accelrys Software Inc., 2012.
- [20] D Schneidman-Duhovny; Y Inbar; R Nussinov, HJ Wolfson, PatchDock and SymmDock: servers for rigid and symmetric docking. *Nucl. Acids. Res.* **2005**, 33, W363-367.
- [21] <http://www.pymol.org/>
- [22] A Tiwari. *Insilico Biol.*, **2007**, 7, 651-661.
- [23] C Perez; M Pauli; P Bazerque. *Acta. Biol. Med. Exp.*, **1990**, 15, 113-115.
- [24] WJ Geary. *Coord. Chem. Rev.*, **1971**, 7, 81.
- [25] S Chandra; D Jain; AK Sharma; P Sharma. *Molecules*, **2009**, 14, 174-190.
- [26] N Raman; S Thalamuthu; J Dhaveethuraja, MA Neelakandan; S Banerjee. *J. Chil. Chem. Soc.*, **2008**, 53, 1439-1443.
- [27] N Dharamaraj; P Viswanathamurthi; K Natarajan. *Trans Met Chem*, **2001**, 26, 105.
- [28] S Belaid; A Landreau; S Djebbar; O Benali-Baitich; G Bouet; JP Bouchara. *J. Inorg. Biochem.* **2008**, 102, 63.